

This is the accepted manuscript made available via CHORUS. The article has been published as:

Unstable flip-flopping spinning binary black holes

Carlos O. Lousto and James Healy

Phys. Rev. D **93**, 124074 — Published 30 June 2016

DOI: [10.1103/PhysRevD.93.124074](https://doi.org/10.1103/PhysRevD.93.124074)

Unstable flip-flopping spinning binary black holes

Carlos O. Lousto and James Healy

*Center for Computational Relativity and Gravitation,
School of Mathematical Sciences, Rochester Institute of Technology,
85 Lomb Memorial Drive, Rochester, New York 14623*

(Dated: June 22, 2016)

We provide a unified description of the flip-flop and the anti-alignment instability effects in spinning black hole binaries in terms of real and imaginary flip-flop frequencies. We find that this instability is only effective for mass ratios $0.5 < q < 1$. We find analytic expressions that determine the region of parameter space for which the instability occurs in terms of maps of the spin magnitudes and mass ratio $(\alpha_1, \alpha_2; q)$. This restricts the priors of parameter estimation techniques for the observation of gravitational waves from quasi-aligned spinning binary black holes and it is relevant for their astrophysical modeling and final recoil computations.

PACS numbers: 04.25.dg, 04.25.Nx, 04.30.Db, 04.70.Bw

I. INTRODUCTION

With advanced LIGO's [1] first detection confirming general relativity's predictions of gravitational waves from the merging of binary black holes (BBH) [2–4] and the beginning of the Gravitational Wave Astronomy era, one of the most important tasks will be to determine the physical parameters of these BBH systems. Highly precessing effects near merger are particularly challenging to model. These effects depend strongly on the spin orientations and magnitudes of each individual black hole.

The strongest dynamical effect of the spins on the orbit of BBH is the hangup effect [5], that depending on the spin components along the orbital angular momentum (aligned or counteraligned) delays or prompts the merger of BBH with respect to the nonspinning case.

Two recent studies shed light on interesting effects of spin precession: i) the individual spin of a black hole may completely flip directions along the orbital angular momentum during the latest inspiral phase of the BBHs [6, 7] and ii) for certain antialigned configurations the black hole spin components along the orbital angular momentum can evolve into large deviations even from small initial angular misalignments [8].

In this letter we provide a unified description of these two phenomena which gives new insight on the origin of the misalignment instability and confirms its existence in higher order post-Newtonian expansions and full numerical simulations. We also discuss some of the consequences of this phenomenon for astrophysical modeling, gravitational waves parameter estimation, and computation of gravitational recoils.

II. POST NEWTONIAN SPIN DYNAMICS

Gerosa et al. [8] have found that a binary black hole configuration with the larger black hole spin α_2 along the orbital angular momentum \vec{L} and the smaller hole spin α_1 counteraligned to it is unstable under polar angular

perturbations when their separation is in between $r_{u\pm} = (\sqrt{\alpha_2} \pm \sqrt{q\alpha_1})^4 M / (1 - q)^2$. This result was found using the orbit averaging approximation [9]. Here we perform a study of these spin dynamics by numerically integrating higher order post-Newtonian (3.5PN) equation of motion and spin evolutions (2.5PN) as given in [10, 11].

Each panel of Fig. 1 displays the results of 121 integrations of the PN spin and equations of motion for a labeled mass ratio $q = m_1/m_2 < 1$ and covering the $-1 \leq \alpha_{1L} \leq 0$ and $0 \leq \alpha_{2L} \leq 1$ quadrant of the aligned spin parameter space (except $q = 0.95$ which has 76 integrations.) The integrations start from quasi-circular orbits at a large enough initial binary separation such that the spins are stable, ie $r > R_c$ given in Eq. (3) (with the total mass of the system $M = m_1 + m_2$), and we stop at a fiducial $r = 11M$, where PN evolutions are still reliable. We choose the spin of the large black hole $\vec{S}_2 = \vec{\alpha}_2 m_2^2$ initially aligned with the orbital angular momentum \vec{L} and the spin of the smaller black hole $\vec{S}_1 = \vec{\alpha}_1 m_1^2$ one degree from exact anti-alignment, i.e. 179 degrees from the \vec{L} -direction (we also verified it for 5 to 30 degrees misalignments). The instability occurs either when the larger or the smaller (or both) black hole spin is slightly misaligned with \vec{L} . The instability depopulates the upper left corner of the spin parameter space, with successively larger portions from $q = 0.5$ to $q = 1$, and strongly changes the spin components along \vec{L} bringing the binary system to strong precession.

From the initially large separations, when the system is stable and spins oscillate at the flip-flop frequency, Ω_{ff} , the binary separation shrinks due to gravitational radiation and eventually reaches a critical separation, see upper panel in Fig. 2. At this point the polar oscillations of the spin begin to grow fast in an out-spiral fashion (see lower panels).

As seen in the middle panels of Fig. 2, the spin misalignment reaches large values at later times (and smaller separations), but the cosine of the angles θ_{1L} and θ_{2L} that the spins form with \vec{L} -direction bare a re-

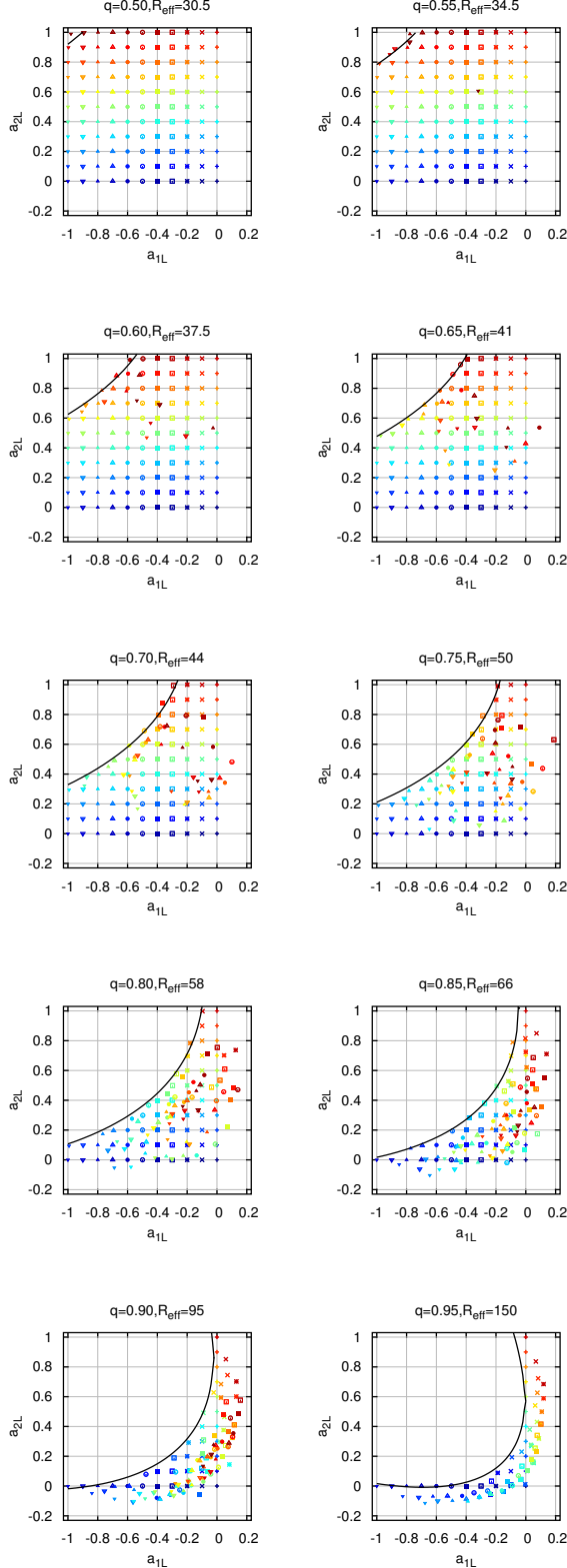


FIG. 1. Snapshots of the spin components along the orbital angular momentum at a binary separation $r/M = 11$. The integration of the PN evolution equations for each binary mass ratio q , started at $r > R_c$ with a uniform distribution of spins in the range $0 \leq \alpha_{2L} \leq 1$ for the large BH and $-1 \leq \alpha_{1L} \leq 0$ for the small BH, which was antialigned with the orbital angular momentum by 179-degrees. The color indicates the original value of the spins. The black curve models the depopulation region as given in Eq. (4).

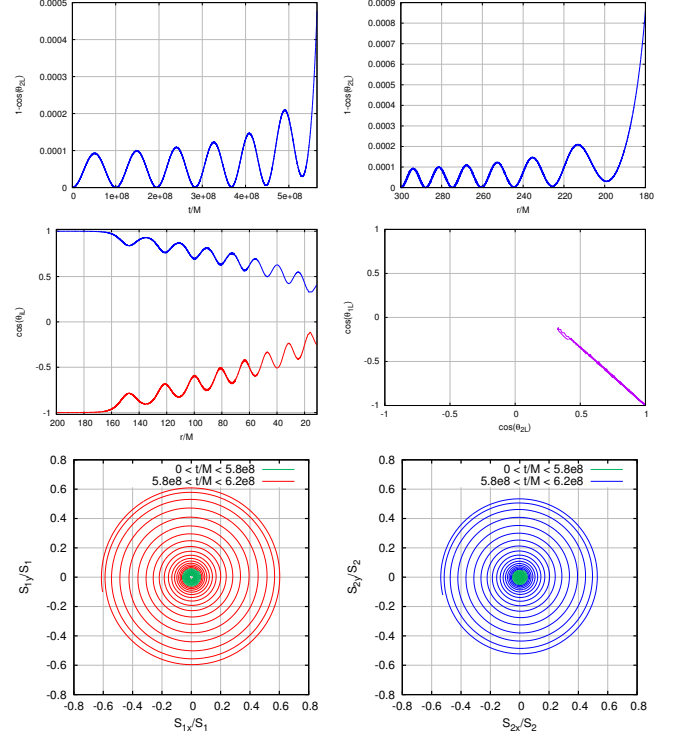


FIG. 2. Evolution of a binary with mass ratio $q = 0.75$, large BH spin $\alpha_{2L} = 1$ initially aligned, and small BH spin $\alpha_{1L} \cong -1$ antialigned with the orbital angular momentum by 179-degrees. The upper panels display the onset of the instability from stable flip-flop oscillations. The middle panels display the development of the instability as the binary separation shrinks. Here $\cos \theta_{iL} = S_{iL}/S_i$ with $i = 1, 2$ for the small, large holes respectively. The lower panels display a polar view of the onset of the misalignment instability.

lation that preserves (mostly) $\vec{S}_0 \cdot \hat{L}$ as expected [12], i.e. $q \cos \theta_{1L} + \cos \theta_{2L} = 1 - q$ for this case with $\alpha_{2L} = 1$ and $\alpha_{1L} \cong -1$.

We will show next that the critical radii separating the two stability regimes can be described in terms of the vanishing of the *flip-flop* frequency Ω_{ff} , separating real and imaginary values, and corresponding to stable and unstable phases respectively.

III. FLIP-FLOP INSTABILITY

In Ref. [7] we give the following expression for the *flip-flop* frequency; the frequency of polar oscillations (with respect to \hat{L}) of the spins in a binary system

$$\begin{aligned} \Omega_{ff}^2 = & \frac{9}{4} \frac{(1-q)^2 M^3}{(1+q)^2 r^5} + 9 \frac{(1-q)(S_{1\hat{L}} - S_{2\hat{L}})M^{3/2}}{(1+q)r^{11/2}} \\ & - \frac{9}{4} \frac{(1-q)(3+5q)S_{1\hat{L}}^2}{q^2 r^6} + \frac{9}{2} \frac{(1-q)^2 S_{1\hat{L}} S_{2\hat{L}}}{qr^6} \quad (1) \\ & + \frac{9}{4} \frac{(1-q)(5+3q)S_{2\hat{L}}^2}{r^6} + \frac{9}{4} \frac{S_0^2}{r^6} + 9 \frac{(1-q)^2 M^4}{(1+q)^2 r^6}, \end{aligned}$$

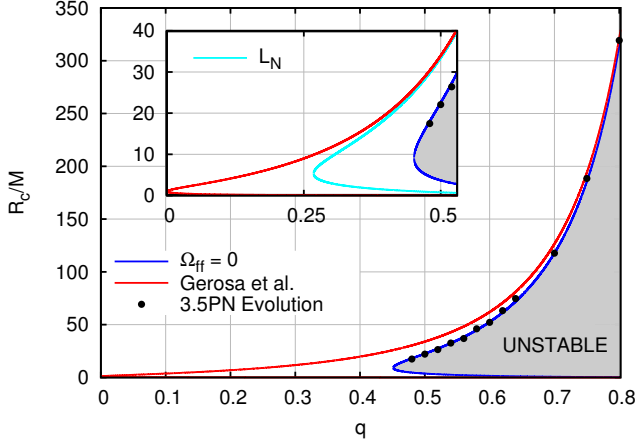


FIG. 3. The instability region, between R_c^\pm , as a function of the mass ratio, q , as the binary transitions from real to imaginary flip-flop frequencies (blue curve) for maximal spins $\alpha_{1L} = -1$ and $\alpha_{2L} = +1$. For comparison also plotted are $r_{ud\pm}$ from [8] (red curve) and use of the reduced to Newtonian order angular momentum L_N (cyan curve in inset) in (A11) of [7]. The dots correspond to 3.5PN evolutions from large initial separations.

where $\vec{S}_0/M^2 = (1+q) [\vec{S}_1/q + \vec{S}_2]$.

The instability of Ref. [8] can be interpreted in terms of an *imaginary flip-flop* frequency, when the oscillations become exponentially growing modes. In fact, we observed in Fig. 2 that, at large separations, the binary oscillates at the frequency given in Eq. (1). Thus, the critical radius, R_c , for which the onset of the instability occurs satisfies

$$\Omega_{ff}(q, \vec{\alpha}_1, \vec{\alpha}_2, R_c) = 0. \quad (2)$$

The solution of this quadratic equation for antialigned spins leads to two roots R_c^\pm .

$$R_c^\pm = 2M \frac{A \pm 2(\alpha_{2L} - q^2 \alpha_{1L})\sqrt{B}}{(1 - q^2)^2}, \quad (3)$$

$$A = (1 + q^2)(\alpha_{2L}^2 + q^2 \alpha_{1L}^2),$$

$$-2q(1 + 4q + q^2)\alpha_{1L}\alpha_{2L} - 2(1 - q^2)^2$$

$$B = 2(1 + q) [(1 - q)q^2 \alpha_{1L}^2 - (1 - q)\alpha_{2L}^2$$

$$- 2q(1 + q)\alpha_{1L}\alpha_{2L} - 2(1 - q)^2(1 + q)].$$

We display these in Fig. 3 for the case of maximally spinning holes, i.e. $\alpha_{1L} \cong -1$ and $\alpha_{2L} = +1$, as a function of the mass ratio q , as this case leads to the most unstable configuration (see Fig. 1). The instability occurs only above a given mass ratio, and in practice this leads to important effects only for $q \gtrsim 1/2$. There is no solution

for instabilities in the other quadrants, thus they only occur when the small black hole is near anti-alignment and the large black hole is near alignment with \vec{L} .

We also verified that the large oscillations shown in the middle panels of Fig. 2, after the instability brought the spins to strong misalignments, are due to the frequency (1) becoming real again, and then back to imaginary successively.

We can now determine analytically the border between stable and unstable configurations in the spin parameter space. For a given q , there is a minimal R_c for which the instability has enough time to act and change notably the components of the spins along \vec{L} . We call this minimal (dimensionless) radius R_{eff} . By inserting $r/M = R_{eff}$ into equation (2) we can solve the resulting quadratic equation for $\alpha_2^B(q, \alpha_{1L}) = \alpha_2^\pm(q, \alpha_{1L}; R_{eff})$

$$\alpha_2^B(q, \alpha_1) = \frac{(1 - q^2)\sqrt{R_{eff}} - q(1 + q^2)\alpha_{1L}}{3 - q^2} \mp \frac{1}{2} \frac{(1 - q^2)}{(3 - q^2)} \sqrt{C}, \quad (4)$$

$$C = 16q^2 \alpha_{1L}^2 - 2(1 - q^2)R_{eff} + 8(q^2 - 3),$$

$$- 8q\sqrt{R_{eff}}(1 + 2q - q^2)\alpha_{1L}/(1 - q).$$

Applying this formula to the border of the depopulated regions in Fig. 1 leads to a simple fit to all q -cases studied here giving $R_{eff} = (25 - 17q)/(1 - q)$. This R_{eff} is larger for $q \sim 1$ than for $q \sim 1/2$ since the smaller the mass ratio the longer it takes radiation reaction to shrink the binary as the energy radiated near merger scales roughly with $\eta^2 = q^2/(1 + q)^4$ [13]. This shows that while the instability acts on the shorter precession time scale, the process of misaligning continues to act on the longer radiation reaction time scale until merger (See Fig. 2).

We note that above $q = 0.85$ the second root α_2^B , begins to also limit the upper part of the panel. In the $q = 1$ limit the two α_2^\pm roots agree, merging into a diagonal straight line $\alpha_{2L} = -\alpha_{1L}$, representing the fact that for $q = 1$, the spins have 180-degrees flip-flop oscillations with $\Omega_{ff}(q = 1) = \frac{3}{2} \frac{S_0}{r^3}$ (see Eq. (2)).

IV. FULL NUMERICAL EVOLUTIONS

Post-Newtonian evolutions do not accurately account for the final plunge, merger and ringdown of binary black holes. We hence stopped our PN evolutions at a fiducial separation of $r = 11M$. We have then performed a few representative full numerical simulations using the techniques in [3] to follow up those post-Newtonian integrations. The parameters of the five continued simulations are given in Table I.

After the completion of the evolution down to merger, the properties of the final black hole remnant are displayed in table II. Notably, the measured recoil velocity is very different from that expected if the spins would remain aligned (this prediction based on the formulae in [13]). The differences are not only due to the magnitude of the recoil, but notably, the velocity component along the original orbital angular momentum, which vanishes for the aligned spins

TABLE I. Initial data parameters and system details for full numerical evolutions. The initial coordinate separation is $D = 11M$ and the intrinsic spins are $\alpha_{1,2}^{x,y,z}$. The eccentricity measured at the end of the inspiral is e_f , and N is the number of orbits just before merger. # labels the PN runs that started at binary separation $r = 500M$ with normalized spins (a_1^z, a_2^z) .

#	(a_1^z, a_2^z)	q	α_1^x	α_1^y	α_1^z	α_2^x	α_2^y	α_2^z	N	e_f
1	$(-0.8, 0.8)$	0.70	0.7738	0.1876	-0.0775	0.6162	0.4183	0.2921	8.7	0.0037
2	$(-0.4, 0.8)$	0.75	-0.3205	0.2392	0.0070	-0.5926	-0.2040	0.4971	9.6	0.0009
3	$(-0.6, 0.6)$	0.75	0.5467	0.2462	-0.0223	0.4724	0.3311	0.1651	8.4	0.0024
4	$(-0.8, 0.8)$	0.75	0.0559	0.7598	-0.2440	-0.2564	0.6676	0.3585	8.6	0.0052
5	$(-0.8, 0.4)$	0.75	-0.4617	-0.4859	-0.4367	0.0581	-0.3765	0.1220	7.4	0.0040

TABLE II. Remnant properties of the merged black hole. The final mass m_{rem} and spin α_{rem} (normalized to total initial mass) are measured from the horizon, and the recoil velocity (in km/s) is calculated from the gravitational waveforms. Comparison with predicted aligned spins values m_{pre} , $\alpha_{pre}^{x,y,z}$, V_{pre}^{xy} , is based on [13]

#	m_{rem}	m_{pre}	α_{rem}^x	α_{rem}^y	α_{rem}^z	α_{pre}^z	V_{rem}^x	V_{rem}^y	V_{rem}^z	V_{pre}^{xy}
1	0.9445	0.9456	0.2577	0.1529	0.7495	0.7742	-3.9	28.7	-133.7	260.7
2	0.9408	0.9409	-0.1868	-0.0322	0.7927	0.7994	273.5	-24.9	-775.8	187.7
3	0.9485	0.9486	0.1945	0.1208	0.7220	0.7388	138.1	-11.2	557.8	200.4
4	0.9468	0.9462	-0.0717	0.2790	0.7537	0.7601	5.9	117.0	241.7	282.9
5	0.9534	0.9546	-0.0639	-0.1565	0.6656	0.6752	47.6	-11.1	386.4	201.7

configuration, now becomes the largest. Differences are also observed in the final spin magnitude and orientation, while the differences in the total energy radiated are less notable.

V. DISCUSSION

We have provided a unified description of the polar oscillations and instabilities of the black hole spins in a binary system. Analytic expressions for the radius of the onset of instabilities and the region of parameter space affected by instabilities are also given. These expressions lead to restrictions of the prior distributions of aligned spins affecting the parameter estimations of gravitational wave observations from binary black holes by removing the unstable region from the posterior probability distributions.

Our study of the onset of instability strictly applies to small (differential) angles deviating from anti-aligned spins with \vec{L} . Notably, we find that this picture remains valid for relatively large angular deviations. The depletion of the upper corner in the $(\alpha_{1L}, \alpha_{2L})$ parameter space, remains true for angles off the \hat{L} -axis of 35, 45, 50-degrees for mass ratios $q = 0.6, 0.75, 0.90$ respectively. Those results are summarized in Fig. 4 by a color map that dissects binaries with different spin components along and perpendicular to \hat{L} at large initial separations and then near merger. The 67,240 evolutions $(41 \times 41 \times 40)$, corresponds to different initial choices of $(\cos \theta_1, \cos \theta_2, \Delta \phi)$. Both black holes are maximally spin-

ning.

These results implies that using (anti-)aligned spin models should remain a good approximation to more general systems for a large portion of the parameter space if the instability depletion is taken into account for quasi-antialigned spins, since the main binary dynamical effect is dominated by the hangup [5] that depends on the spin components along \hat{L} .

In a scenario where accretion [14, 15] nearly anti-align spinning binaries at large separations, the spin instabilities studied here may lead to larger gravitational recoils than expected from their almost counteraligned precursors, leading to black hole remnants with thousand of km/s recoil velocities.

ACKNOWLEDGMENTS

The authors would like to thank M. Campanelli, B. Farr, H. Nakano, V. Raymond, R. O’Shaughnessy, and Y. Zlochower for comments on the original manuscript. Authors also gratefully acknowledge the NSF for financial support from Grant PHY-1305730. Computational resources were provided by XSEDE allocation TG-PHY060027N, and by the BlueSky Cluster at Rochester Institute of Technology, which were supported by NSF grant No. AST-1028087, and PHY-1229173.

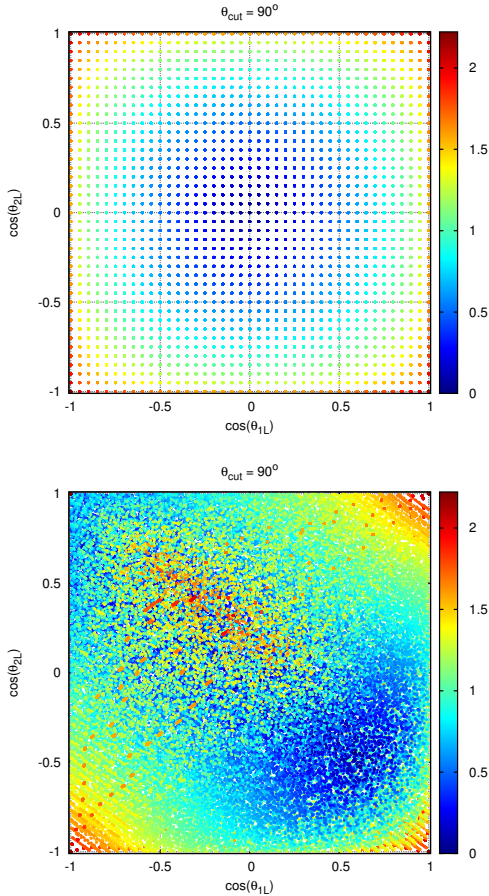


FIG. 4. Upper: Initial configuration of a binary with mass ratio $q = 0.75$ at $r = 500M$ of separation. Color labels angular deviations of the spins from the orbital angular momentum direction \hat{L} . Lower: The spin orientations near merger at $r = 11M$ displaying a replenish of the unstable region from the highly misaligned spins.

-
- [1] B. Abbott *et al.* (Virgo, LIGO Scientific), Phys. Rev. Lett. **116**, 061102 (2016), arXiv:1602.03837 [gr-qc].
 - [2] F. Pretorius, Phys. Rev. Lett. **95**, 121101 (2005), gr-qc/0507014.
 - [3] M. Campanelli, C. O. Lousto, P. Marronetti, and Y. Zlochower, Phys. Rev. Lett. **96**, 111101 (2006), gr-qc/0511048.
 - [4] J. G. Baker, J. Centrella, D.-I. Choi, M. Koppitz, and J. van Meter, Phys. Rev. Lett. **96**, 111102 (2006), gr-qc/0511103.
 - [5] M. Campanelli, C. O. Lousto, and Y. Zlochower, Phys. Rev. **D74**, 041501(R) (2006), gr-qc/0604012.
 - [6] C. O. Lousto and J. Healy, Phys. Rev. Lett. **114**, 141101 (2015), arXiv:1410.3830 [gr-qc].
 - [7] C. O. Lousto, J. Healy, and H. Nakano, Phys. Rev. **D93**, 044031 (2016), arXiv:1506.04768 [gr-qc].
 - [8] D. Gerosa, M. Kesden, R. O'Shaughnessy, A. Klein, E. Berti, U. Sperhake, and D. Trifirò, Phys. Rev. Lett. **115**, 141102 (2015), arXiv:1506.09116 [gr-qc].
 - [9] J. D. Schnittman, Phys. Rev. **D70**, 124020 (2004), arXiv:astro-ph/0409174.
 - [10] T. Damour, P. Jaranowski, and G. Schafer, Phys. Rev. **D77**, 064032 (2008), arXiv:0711.1048 [gr-qc].
 - [11] A. Buonanno, Y. Chen, and T. Damour, Phys. Rev. **D74**, 104005 (2006), gr-qc/0508067.
 - [12] E. Racine, Phys. Rev. **D78**, 044021 (2008), arXiv:0803.1820 [gr-qc].
 - [13] J. Healy, C. O. Lousto, and Y. Zlochower, Phys. Rev. **D90**, 104004 (2014), arXiv:1406.7295 [gr-qc].
 - [14] T. Bogdanović, C. S. Reynolds, and M. C. Miller, Astrophys. J. **661**, L147 (2007), arXiv:astro-ph/0703054.
 - [15] M. Coleman Miller and J. H. Krolik, Astrophys. J. **774**, 43 (2013), arXiv:1307.6569 [astro-ph.HE].